

## Oral mucosa optical biopsy by a novel handheld fluorescent confocal microscope specifically developed: technologic improvements and future prospects

Maria Contaldo, DMD, PhD,<sup>a</sup> Catherine F. Poh, DMD, PhD,<sup>b</sup> Martial Guillaud, PhD,<sup>b</sup> Alberta Lucchese, DMD, PhD,<sup>a</sup> Rosario Rullo, MD,<sup>a</sup> Sylvia Lam, PhD,<sup>b</sup> Rosario Serpico, MD,<sup>a</sup> Calum E. MacAulay, PhD,<sup>b</sup> and Pierre M. Lane, PEng, PhD<sup>b</sup>  
Second University of Naples, Naples, Italy; British Columbia Cancer Agency, Vancouver, BC, Canada

**Objective.** This pilot study evaluated the baseline effectiveness of a novel handheld fluorescent confocal microscope (FCM) specifically developed for oral mucosa imaging and compared the results with the literature.

**Study Design.** Four different oral sites (covering the mucosa of the lip and of the ventral tongue, the masticatory mucosa of the gingiva, and the specialized mucosa of the dorsal tongue) in 6 healthy nonsmokers were imaged by an FCM made up of a confocal fiberoptic probe ergonomically designed for in vivo oral examination, using light at the wavelength of 457 nm able to excite the fluorophore acriflavine hydrochloride, topically administered. In total, 24 mucosal areas were examined.

**Results.** The FCM was able to distinctly define epithelial cells, bacterial plaque, and inflammatory cells and to image submucosal structures by detecting their intrinsic fluorescence.

**Conclusions.** When compared with other devices, this FCM allowed the user to image each oral site at higher magnification, thus resulting in a clearer view. (Oral Surg Oral Med Oral Pathol Oral Radiol 2013;116:752-758)

To date, the diagnosis of suspicious or equivocal oral lesions is based on their conventional clinical examination and confirmed by the histopathologic report subsequent to a mandatory biopsy.<sup>1</sup> Diagnostic procedures can benefit from adjunctive tools. Among these, tissue autofluorescence visualization<sup>2-5</sup> and toluidine blue<sup>6</sup> and Lugol iodine vital staining<sup>7</sup> have been used to improve the ability to screen and clinically identify oral premalignant and malignant lesions in order to facilitate the diagnostic pathway<sup>8</sup> in a noninvasive, real-time way.

Biopsy providing definitive microscopic features remains the gold standard for the management of lesions with high-grade dysplasia or greater tissue change, which require treatment, and those with low-grade dysplasia that will usually be monitored over time with periodic comparative biopsies. As a surgical procedure, biopsy is invasive, and the selection of the biopsy site can be problematic. In a large lesion, multiple biopsies might be necessary for a more accurate histopathologic analysis; for areas with posttreatment mucosal change, repeated and excisional biopsies can cause more problems. It is acceptable to resect a relatively large area (approximately 1 to 2 cm) of normal-appearing mucosa around the visibly abnormal lesion to compensate for the limitation of the surgeon's ability to exactly

determine the margins of carcinoma or dysplasia<sup>9</sup>; this approach produces better likelihood of complete excision but increases postoperative discomfort, thus resulting in low compliance among the patients, who may become reluctant to perform further follow-up biopsies. Noninvasive approaches that can help the clinicians to decide the timing and the best site for a diagnostic biopsy and to avoid unnecessary biopsies are needed.

Optical imaging technologies have shown promise in meeting that need. In vivo confocal microscopy, one such optical technology, has been widely used to investigate the tissue at microscopic resolution in a real-time fashion in clinical settings, such as ophthalmology,<sup>10</sup> dermatology,<sup>11,12</sup> gynecology,<sup>13-16</sup> and gastroenterology.<sup>17-19</sup> Due to its noninvasiveness and its time-saving nature, it could be advantageously performed at the point of care.

The application of confocal microscopy in the oral cavity is limited to some preliminary work previously reported.<sup>20-23</sup> Detailed descriptions of "confocal criteria" of healthy oral structures also appeared in

### Statement of Clinical Relevance

The results represent a major technical advance in the development of this optical imaging modality for the in vivo oral mucosa examination, thus allowing examination of each site of the oral mucosa for cellular details during an otherwise routine examination.

<sup>a</sup>Multidisciplinary Department of Medical-Surgical and Odontostomatological Specialties, Second University of Naples.

<sup>b</sup>Department Of Integrative Oncology, Research Centre, British Columbia Cancer Agency.

Received for publication Jul 3, 2013; returned for revision Aug 22, 2013; accepted for publication Sep 8, 2013.

© 2013 Elsevier Inc. All rights reserved.

2212-4403/\$ - see front matter

<http://dx.doi.org/10.1016/j.oooo.2013.09.006>

further works, adapting confocal microscopes designed for dermatologic use to be used in the oral cavity.<sup>24,25</sup>

The objectives of this pilot study were to image healthy oral mucosa to evaluate the baseline effectiveness of an easy-to-use, handheld fluorescent confocal microscope (FCM) specifically developed for in vivo oral evaluation and to criticize and compare results with previous works.

## SUBJECTS AND METHODS

### Subjects

Six healthy nonsmokers were enrolled at the Imaging Unit in the Department of Integrative Oncology of the British Columbia Cancer Agency of Vancouver, BC, Canada, after informed and written consent. The study was approved by the Institutional Research Board of the BC Cancer Agency/University of British Columbia (H11-00011). The series comprised 4 men and 2 women (mean age,  $29.6 \pm 4.6$  years) without any oral mucosal conditions. They were subjected to FCM examination (see below for instrumentation) of different oral mucosal sites. In total, 24 mucosal areas were examined, as follows: 6 labial mucosae and 6 ventral surfaces of the tongue, 6 attached gingivae, and 6 dorsal surfaces of the tongue. The former 2 sites were used to represent non-keratinized oral mucosa; the gingiva was used as a keratinized one; and the dorsal surface represented the specialized epithelium. Because the present work is a pilot study to define quality of images and details, comparing them with previous works, biopsies were not performed.

### In vivo FCM

Fluorescence confocal microscopy is an imaging technique based on the detection of fluorescent light emitted by an endogenous marker or an exogenous substance applied to the living tissue when illuminated by a specific wavelength. This work examines a prototype of a handheld fluorescent confocal microscope, specifically developed for oral examinations (BC Cancer Agency, Imaging Unit, Integrative Oncology, Vancouver, BC, Canada). The system was based on previously reported laser-scanning designs.<sup>22,26</sup> The handheld wand employed a custom (7-element)  $3 \times /1.0$  numerical aperture objective lens with a 240- $\mu\text{m}$  field of view. Blue excitation light was provided by a 457-nm laser diode (Melles Griot, Carlsbad, CA, USA). Reflected excitation was blocked by a 475-nm long-pass filter (Chroma Technology, Bellows Falls, VT, USA), thus allowing detection of the fluorescence emitted by acriflavine hydrochloride (AH) as a contrast agent topically applied to the mucosal surface.<sup>22</sup> AH and its derivatives have been previously used for fluorescence imaging in the European, Asian, and Australian gastrointestinal literature without any adverse effects noted,<sup>18</sup> and El

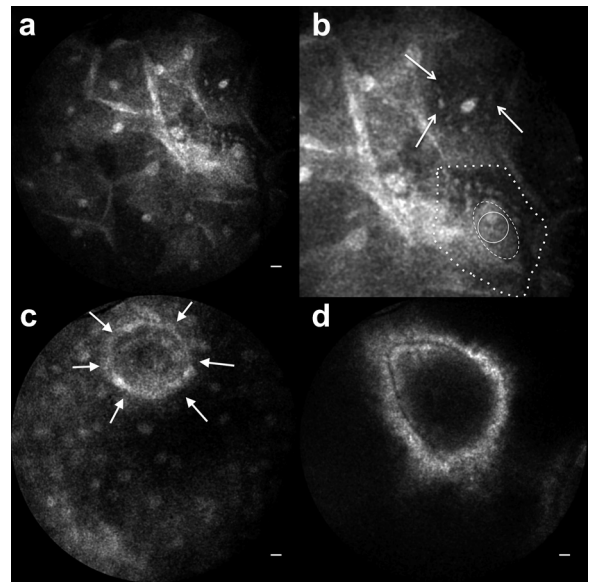


Fig. 1. Lip imaging with a fluorescent confocal microscope. (a) Keratinocytes appear as plump, roundish cells, defined by bright boundaries, gray cytoplasm, and a central strongly bright nucleolus surrounded by a dark nuclear halo. (b) Detail of the squared selection in (a), showing 2 keratinocytes with perinuclear granules (white arrows) and whose contours, perinuclear granules, and nucleolus are marked by dotted lines from outer to inner. (c) At the lowest epithelial layers, some roundish structures (white arrows), made up by cells organized in a bright ring, resemble a minor salivary gland duct. (d) The dark ring surrounded by a bright halo corresponds to a connective tissue papilla limited by epithelium. Scale bars, 10  $\mu\text{m}$ .

Hallani et al.<sup>27</sup> found AH to be the best contrast agent when compared with other types, thus supporting our choice.

### FCM acquisition method

After the application of 0.05% AH on the mucosal surface for 5 minutes, the volunteer washed out the excess using water; then FCM examination took place. En face, single,  $240 \times 240$ - $\mu\text{m}$  FCM images and videos were collected from each mucosal layer of the different mucosal subtypes (covering, masticatory, and specialized mucosa), starting from the most superficial visible layer of the tissue and progressing to the deepest visible layer.

Because the FCM probe was still being modified at the time of this study, the imaging depth could not be accurately and quantitatively determined. For these reasons, based on the knowledge gained in reflectance confocal microscopy imaging,<sup>24</sup> the imaged layers were conventionally classified on the basis of their appearance as follows: superficial layer, related to the first layers of keratinocytes; stratum spinosum, corresponding to the homonymous histologic layer; lower layer, corresponding

**Table I.** Oral mucosa cellular and architectural features observed in each subsite

	<i>Superficial layer</i>	<i>Stratum spinosum</i>	<i>Lower layer</i>	<i>Submucosa</i>
Nonkeratinized mucosa	<ul style="list-style-type: none"> <li>- plump round/oval cells</li> <li>- bright nucleolus</li> <li>- nuclear dark halo</li> <li>- perinuclear granules</li> <li>- pale gray cytoplasm</li> <li>- thin, bright cell boundaries</li> </ul>	<ul style="list-style-type: none"> <li>- progressive reduction in size of keratinocytes</li> <li>- frosted-glass pattern</li> </ul>	<ul style="list-style-type: none"> <li>- salivary gland ducts</li> <li>- regular epithelial-connective tissue interdigitation</li> <li>- target-like structures (horizontal blood vessels within connective tissue)</li> </ul>	<ul style="list-style-type: none"> <li>- horizontal blood vessels</li> <li>- fibroblasts</li> <li>- collagen bundles</li> <li>- skeletal muscles</li> </ul>
Masticatory mucosa	<ul style="list-style-type: none"> <li>- isolated polygonal corneocytes</li> <li>- strongly gray cytoplasm</li> <li>- bright nucleolus</li> <li>- dark nuclear halo</li> </ul>	<ul style="list-style-type: none"> <li>- eye-shaped small keratinocytes strongly attached to each other</li> <li>- strong, bright cell boundaries</li> </ul>	<ul style="list-style-type: none"> <li>- epithelial cells not individually identifiable</li> <li>- high epithelial—connective tissue interdigitation</li> </ul>	<ul style="list-style-type: none"> <li>- grayish-to-black subepithelial tissue</li> </ul>
Specialized mucosa	<ul style="list-style-type: none"> <li>- filiform papillae</li> <li>- fungiform papillae</li> </ul>	<ul style="list-style-type: none"> <li>- keratinocytes fitted together</li> <li>- comma-like nucleolus</li> <li>- pale dark nuclear halo</li> <li>- gray cytoplasm</li> <li>- tile/puzzle pattern</li> </ul>	<ul style="list-style-type: none"> <li>- strong marked epithelial—connective tissue interdigitation</li> </ul>	<ul style="list-style-type: none"> <li>- grayish-to-black subepithelial tissue</li> </ul>

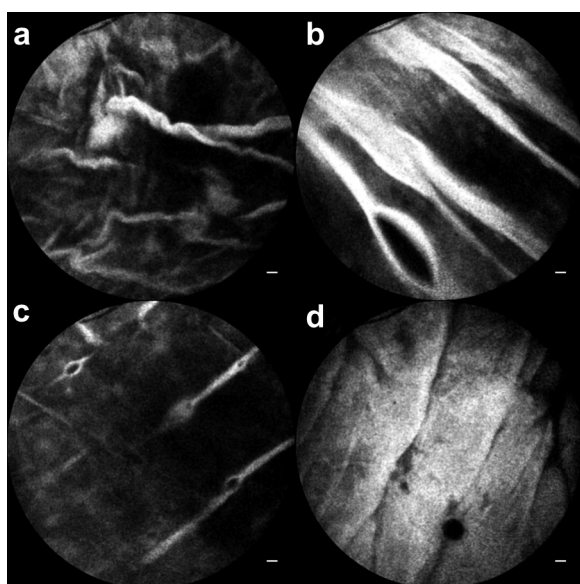


Fig. 2. Ventral tongue imaging with a fluorescent confocal microscope. Details of the submucosal structures imaged in the ventral tongue. (a) Blood vessels below the epithelium are recognized because of their regular and waved shape. (b) Highly fluorescent collagen bundles, visible as linear thick structures parallel to each other. (c) Fibroblasts. (d) Highly fluorescent masses, identified as skeletal muscles. Scale bars, 10  $\mu$ m.

to the epithelial—connective tissue junction; and submucosa. The videos collected have been displayed as single frames to allow analysis of each of them as a single image.

**RESULTS**

**Nonkeratinized mucosa**

*Labial mucosa.* From the surface to the stratum spinosum, the keratinocytes appeared as big, plump, roundish cells, well defined with a clear cell-to-cell

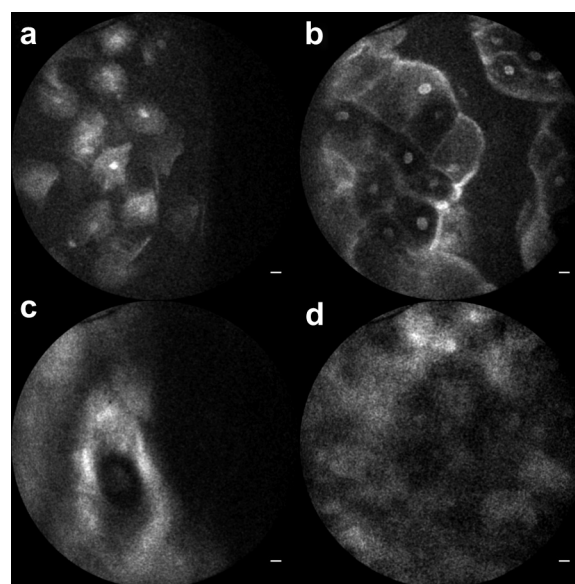


Fig. 3. Gingival imaging with a fluorescent confocal microscope. (a) Superficial keratinized layer shows isolated cells with pyknotic nuclear material and polygonal contours. (b) Below the surface, gingival eye-shaped cells are in close contact and show hyperfluorescent boundaries and a central bright nucleus surrounded by a darker nuclear halo. At the epithelial—connective tissue junction, connective tissue is partly well encircled by bright epithelial rings (c) and partly visible in an alternated dark-gray pattern (d), because of their strong interdigitation. Scale bars, 10  $\mu$ m.

border and a centrally located roundish bright nucleolus<sup>28</sup> limited by a perinuclear dark zone, surrounded by brighter smaller bodies within a pale gray cytoplasm (Figure 1, a and b; Table I). They were arranged in a frosted glass—like pattern.<sup>24</sup>

At the lowest epithelial layers, some concentric circular structures delimited by a bright ring may correspond

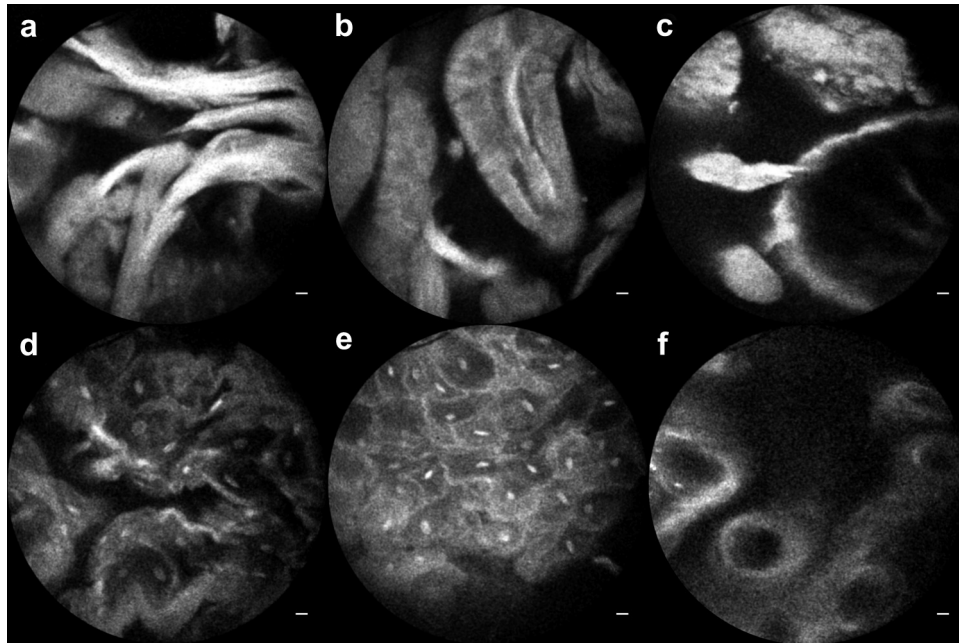


Fig. 4. Dorsal tongue imaging with a fluorescent confocal microscope. Filiform papillae are highly fluorescent and well identifiable by their characteristic shape, completely bright when imaged at their outer surface (a), and with a central, linear, bright core distinguishable from the remaining gray body (b) when focusing on their inner section. (c) Fungiform papillae are imaged as roundish islands of grayish tissue with strong contours. (d) The macroscopic papillary surface of the dorsal tongue is well represented at the microscopic level on fluorescent confocal microscope examination by the alternation between cellular layers and dark areas. (e) At the stratum spinosum, cells are arranged in a “tile/puzzle pattern” with bright nongeometric outlines, fitted together, rich in gray cytoplasm and comma nucleoli, with a pale dark nuclear halo. (f) The epithelial–connective tissue junction was represented by a bright ring, corresponding to the epithelial layer, encircling a dark area inside, representing the connective tissue. Scale bars, 10  $\mu$ m.

to the minor salivary gland ducts (see Figure 1, c). Epithelial–connective tissue papillae were recognizable because of the presence of a dark ring surrounded by a bright halo (see Figure 1, d).

**Ventral tongue mucosa.** Ventral tongue mucosa appeared to be predominantly constituted by large oval cells with well-defined hyperreflecting borders. Similarly to those in the labial mucosa, described earlier, keratinocytes were represented by a bright roundish nucleolus, surrounded by a dark nuclear halo. At the stratum spinosum, keratinocytes were smaller than in covering mucosa, and cell boundaries were clearly bright. Epithelial–connective tissue papillae were recognizable because of the presence of dark areas corresponding to the connective tissue, which interdigitates with the surrounding gray epithelium. “Target” structures made up by alternation of bright and dark rings corresponded to the connective tissue papillae (dark rings) centered by horizontal blood vessels (bright rings). Below the epithelium, the blood vessels and the capillary loops appeared very bright and regularly disposed (Figure 2, a). In the deepest frames, very bright, linear, thick structures paralleled each other and corresponded to collagen bundles (see Figure 2, b).

Structures resembling fibroblasts (see Figure 2, c) and skeletal muscles (see Figure 2, d) were also identifiable at the deepest levels. Here, without AH staining, the cellular nucleoli turned dark, whereas collagen fibers, and skeletal muscles turned bright owing to their intrinsic fluorescent property (autofluorescence).

### Masticatory mucosa

**Attached gingiva.** In gingiva, superficial keratinization was expressed by the presence of very bright keratinocytes appearing as isolated singular cells, floating like in a cytology smear and showing well-defined outlines, strongly gray cytoplasm, and bright nucleoli (Figure 3, a). Below the surface, cells were elongated and “eye-shaped,” with bright roundish nucleoli and a dark nuclear halo (see Figure 3, b), whereas the intercellular spaces appeared very bright.

As in other sites, in the lowest stratum spinosum, close to the epithelial–connective tissue junction, the cells did not show well-marked bright outline, but their boundaries were recognizable by contrast between gray cytoplasm and darker surroundings. Numerous target-like

structures, with alternation of bright and dark roundish concentric rings, were seen (see Figure 3, c).

At the lower layers, large grainy irregular areas without recognizable cells and surrounded by dark areas expressed the pits and crest of the gingival surface (see Figure 3, d).

### Specialized mucosa

**Dorsal tongue.** Filiform and fungiform papillae were identified in lingual specialized epithelium. Filiform papillae were visible thanks to their flexible and elongated shapes. They appeared totally bright when their surface was imaged (Figure 4, a), whereas when the focus was on their inner section, a central linear bright core was distinguished from the remaining gray body (see Figure 4, b). Fungiform papillae were imaged as roundish squat islands of grayish tissue limited by bright contours and separated from each other by dark clefts (see Figure 4, c).

The macroscopic papillary surface of the dorsal tongue was well represented at the microscopic level on FCM examination by the alternation between cellular layers and dark clefts (see Figure 4, d).

The cells at the stratum spinosum were arranged in a “tile/puzzle pattern” with bright nongeometric outlines, fitted together, rich in a gray cytoplasm and comma-like nucleolus, with a very pale dark nuclear halo (see Figure 4, d and e). Big black oval areas, well marked by a bright ring, corresponded to the epithelial–connective tissue junction.

### Bacterial plaque

Both on superficial layers of gingiva and on dorsal tongue, highly bright structures, comma-shaped, roundish, or elongated, densely crowded and surrounded by gray irregular areas, were visible. These bodies resembled bacterial aggregate (singular spheroid- or rod-shaped bacteria and chain aggregate groups) and inflammatory cells. Although they were similar to nucleoli, their shape was not perfectly roundish, and they were not surrounded by uniformly gray cytoplasm and dark nuclear halos, thus differentiating them from nucleoli (Figure 5).

### DISCUSSION

An FCM allows in vivo imaging of the tissue in a noninvasive, real-time way, thus offering histologic details of the tissue analyzed. The development of an FCM specifically for oral imaging could help the clinical approach to diagnosis of precancerous and early cancerous lesions in a time-saving and noninvasive procedure. In the present study, we tested a focusable prototype of an FCM specifically developed for oral

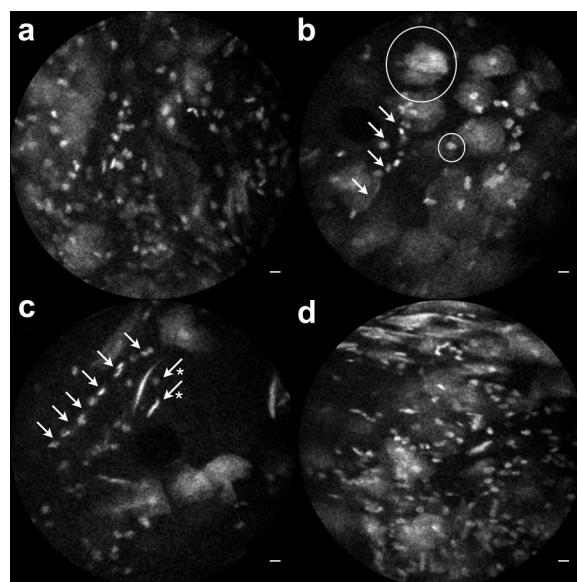


Fig. 5. Bacterial plaque imaging with a fluorescent confocal microscope. (a to d) Small, irregularly roundish, bright bodies are dispersed in a disorderly way among the superficial keratinocytes (whose differences in size are highlighted by the white circles in b). In some points they seem to aggregate in chains (white arrows in b and c), whereas elsewhere they appear as rod-like bodies (white arrows with asterisks in c). Scale bars, 10  $\mu$ m.

cavity access in order to preliminarily establish its suitability to image and define oral mucosal microscopic and architectural features site-by-site, and we compared the results with previous literature.

Data obtained from this analysis showed well-defined images of keratinocytes, layer after layer from surface to submucosa. Compared with an analogous previous study of healthy oral mucosa in vivo imaging obtained by using a reflectance confocal microscope,<sup>24</sup> in the present study the gingival surface appeared more clearly identifiable, and the superficial keratinization did not disturb the light transmission and the fluorescence detection. This evidence may be due to the higher FCM magnification. Furthermore, our FCM was also able to detect dental plaque and bacterial aggregation onto the gingival and dorsal tongue surface, similar to that reported by Dige et al.<sup>29</sup> and Tomás et al.,<sup>30</sup> and subepithelial structures such as blood vessels, connective fibers, and the skeletal muscles, which were previously imaged in an ex vivo way by White et al.<sup>31</sup> with a reflectance confocal microscope. Findings such as the skeletal muscle and the fibroblasts, in this study visible in the ventral tongue because of its thinness, have been imaged in vivo here for the first time, due to the intrinsic fluorescent properties (autofluorescence) of these structures.

The advantages of the FCM prototype used in our present work, compared with the prior studies, can be summarized as higher resolution, better ergonomics (specifically developed to reach each intraoral site), and the capability to image subepithelial connective structures such as skeletal muscles and fibroblasts, owing to their intrinsic fluorescence detected by the device. Previous studies<sup>32-35</sup> stated that the maximum depth of 150  $\mu\text{m}$  in FCMs is related to the limit of the penetration through the tissues of AH, the fluorophore used in the present and prior studies, whereas reflectance confocal microscopes generally can image to 300  $\mu\text{m}$ , although the quality of images at the deepest layers (submucosa) may be invalidated by the strong light backscattering.

In the present work, we were able to image the deeper structures of covering mucosa well, owing to their intrinsic fluorescence, which our device has been able to detect.

The encouraging results reported, in addition to the good quality of cellular details and to the capability of detecting structures smaller than human cells, such as various bacteria, allow us to define this pilot study as a starting point to encourage further improvements of the device and additional extended studies in vivo on precancerous lesions and early cancers, in order to define criteria of malignancy adequate to perform a correct diagnosis on the sole basis of the in vivo confocal analysis, thus avoiding incisional biopsy and reducing the time required for diagnosis. However, further efforts are required to accurately assess and standardize the depth of imaging, here indirectly and approximately defined, and further comparative analyses among different diseases and conditions affecting the oral cavity and healthy mucosae may shed light on the value of this handheld in vivo tool to be used in clinical settings. Based on its comparative and preliminary nature, the present study did not involve performing biopsies. Once depth of imaging is quantitatively defined, future studies should compare healthy and diseased sites both by in vivo FCM imaging and by gold standard biopsy.

In vivo FCM could also be used to evaluate human papillomavirus-related lesions, which have been found to be related to a fraction of oral squamous cell carcinomas (OSCCs),<sup>36</sup> and further studies may correlate the confocal pattern of the primary tumor with the nodal metastases' features.<sup>37-39</sup> In conclusion, the development of this device, specifically built to be adapted to oral cavity imaging, allows us to overcome the limitations of other commercially available devices that were adaptable but not specific to the stomatologist's area of interest, thus also allowing us to image anatomic areas that are difficult to reach but often affected by OSCC and other diseases, such as the retromolar trigone and

hard palate, whose investigation was previously prevented by unsuitable device ergonomics.

## REFERENCES

1. British Columbia Oral Cancer Prevention Program, BC Cancer Agency; College of Dental Surgeons of British Columbia. Guideline for the early detection of oral cancer in British Columbia. *J Can Dent Assoc.* 2008;74:245.
2. Rosin MP, Poh CF, Guillard M, Williams PM, Zhang L, MacAulay C. Visualization and other emerging technologies as change makers for oral cancer prevention. *Ann N Y Acad Sci.* 2007;1098:167-183.
3. Poh CF, Zhang L, Anderson DW, et al. Fluorescence visualization detection of field alterations in tumor margins of oral cancer patients. *Clin Cancer Res.* 2006;12:6716-6722.
4. Farah CS, Mcintosh L, Georgiou A, McCullough MJ. Efficacy of tissue autofluorescence imaging (velscope) in the visualization of oral mucosal lesions. *Head Neck.* 2012;34:856-862.
5. Scheer M, Neugebauer J, Derman A, Fuss J, Drebber U, Zoeller JE. Autofluorescence imaging of potentially malignant mucosa lesions. *Oral Surg Oral Med Oral Pathol Oral Radiol Endod.* 2006;111:568-577.
6. Cancela-Rodríguez P, Cerero-Lapiedra R, Esparza-Gómez G, Llamas-Martínez S, Warnakulasuriya S. The use of toluidine blue in the detection of pre-malignant and malignant oral lesions. *J Oral Pathol Med.* 2011;40:300-304.
7. Petruzzi M, Lucchese A, Baldoni E, Grassi FR, Serpico R. Use of Lugol's iodine in oral cancer diagnosis: an overview. *Oral Oncol.* 2010;46:811-813.
8. Huber MA. Adjunctive diagnostic aids in oral cancer screening: an update. *Tex Dent J.* 2012;129:471-480.
9. Clark AL, Gillenwater AM, Collier TG, Alizadeh-Naderi R, El-Naggar AK, Richards-Kortum RR. Confocal microscopy for real-time detection of oral cavity neoplasia. *Clin Cancer Res.* 2003;9:4714-4721.
10. Cavanagh HD, Petroll WM, Alizadeh H, He YG, McCulley JP, Jester JV. Clinical and diagnostic use of in vivo confocal microscopy in patients with corneal disease. *Ophthalmology.* 1993;100:1444-1454.
11. Rajadhyaksha M, González S, Zavislan JM, Anderson RR, Webb RH. In vivo confocal scanning laser microscopy of human skin, II: advances in instrumentation and comparison with histology. *J Invest Dermatol.* 1999;113:293-303.
12. Moscarella E, González S, Agazzino M, et al. Pilot study on reflectance confocal microscopy imaging of lichen planus: a real-time, non-invasive aid for clinical diagnosis. *J Eur Acad Dermatol Venereol.* 2012;26:1258-1265.
13. Tan J, Quinn MA, Pyman JM, Delaney PM, McLaren WJ. Detection of cervical intraepithelial neoplasia in vivo using confocal endomicroscopy. *BJOG.* 2009;116:1663-1670.
14. Luck BL, Carlson KD, Bovik AC, Richards-Kortum RR. An image model and segmentation algorithm for reflectance confocal images of in vivo cervical tissue. *IEEE Trans Image Process.* 2005;14:1265-1276.
15. Sung KB, Richards-Kortum R, Follen M, Malpica A, Liang C, Descour M. Fiber optic confocal reflectance microscopy: a new real-time technique to view nuclear morphology in cervical squamous epithelium in vivo. *Opt Express.* 2003;11:3171-3181.
16. Drezek RA, Richards-Kortum R, Brewer MA, et al. Optical imaging of the cervix. *Cancer.* 2003;98(9 suppl):2015-2027.
17. Just T, Stave J, Bombor I, Kreutzer HJ, Guthoff R, Pau HW. In vivo diagnosis of epithelial changes of the oropharynx using confocal microscopy. *Laryngorhinootologie.* 2008;87:174-180.

18. Polglase AL, McLaren WJ, Skinner SA, Kiesslich R, Neurath MF, Delaney PM. A fluorescence confocal endomicroscope for in vivo microscopy of the upper- and the lower-GI tract. *Gastrointest Endosc*. 2005;62:686-695.
19. Polglase AL, McLaren WJ, Delaney PM. Pentax confocal endomicroscope: a novel imaging device for in vivo histology of the upper and lower gastrointestinal tract. *Expert Rev Med Devices*. 2006;3:549-556.
20. White WM, Rajadhyaksha M, González S, Fabian RL, Anderson RR. Noninvasive imaging of human oral mucosa in vivo by confocal reflectance microscopy. *Laryngoscope*. 1999;109:1709-1717.
21. Just T, Stave J, Pau HW, Guthoff R. In vivo observation of papillae of the human tongue using confocal laser scanning microscopy. *ORL J Otorhinolaryngol Relat Spec*. 2005;67:207-212.
22. Muldoon TJ, Roblyer D, Williams MD, Stepanek VM, Richards-Kortum R, Gillenwater AM. Noninvasive imaging of oral neoplasia with a high-resolution fiber-optic microendoscope. *Head Neck*. 2012;34:305-312.
23. Roblyer D, Richards-Kortum R, Kurachi C, Sokolov K. A multi-spectral optical imaging device for in vivo detection of oral neoplasia. *J Biomed Opt*. 2008;13:024019.
24. Contaldo M, Agozzino M, Moscarella E, Esposito S, Serpico R, Ardigò M. In vivo characterization of healthy oral mucosa by reflectance confocal microscopy: a translational research for optical biopsy. *Ultrastruct Pathol*. 2013;37:151-158.
25. Contaldo M, Serpico R, Lucchese A. In vivo imaging of enamel by reflectance confocal microscopy (RCM): non-invasive analysis of dental surface. *Odontology*. 2013. <http://dx.doi.org/10.1007/s10266-013-0110-9>.
26. Lane PM, Lam S, McWilliams A, Leriche JC, Anderson MW, Macaulay CE. Confocal fluorescence microendoscopy of bronchial epithelium. *J Biomed Opt*. 2009;14:024008.
27. El Hallani S, Poh CF, Macaulay CE, Follen M, Guillaud M, Lane P. Ex vivo confocal imaging with contrast agents for the detection of oral potentially malignant lesions. *Oral Oncol*. 2013;49:582-590.
28. Tchélidzé P, Chatron-Colliet A, Thiry M, Lalun N, Bobichon H, Ploton D. Tomography of the cell nucleus using confocal microscopy and medium voltage electron microscopy. *Crit Rev Oncol Hematol*. 2009;69:127-143.
29. Dige I, Nilsson H, Kilian M, Nyvad B. In situ identification of streptococci and other bacteria in initial dental biofilm by confocal laser scanning microscopy and fluorescence in situ hybridization. *Eur J Oral*. 2007;115:459-467.
30. Tomás I, Henderson B, Diz P, Donos N. In vivo oral biofilm analysis by confocal laser scanning microscopy: methodological approaches. In: Méndez-Vilas A, Díaz J, eds. *Microscopy: Science, Technology, Applications and Education*. Badajoz, Spain: Formatex; 2010. Available at: <http://www.formatex.info/microscopy4/597-606.pdf>.
31. White WM, Baldassano M, Rajadhyaksha M, et al. Confocal reflectance imaging of head and neck surgical specimens. A comparison with histologic analysis. *Arch Otolaryngol Head Neck Surg*. 2004;130:923-928.
32. Smithpeter CL, Dunn AK, Welch AJ, Richards-Kortum R. Penetration depth limits of in vivo confocal reflectance imaging. *Appl Opt*. 1998;37:2749-2754.
33. Luedtke MA, Papazoglou E, Neidrauer M, Kollias N. Wavelength effects on contrast observed with reflectance in vivo confocal laser scanning microscopy. *Skin Res Technol*. 2009;15:482-488.
34. Anderson RR, Parrish JA. The optics of human skin. *J Invest Dermatol*. 1981;77:13-19.
35. Carignan CS, Yagi Y. Optical endomicroscopy and the road to real-time, in vivo pathology: present and future. *Diagn Pathol*. 2012;7:98.
36. Pannone G, Santoro A, Carinci F, et al. Double demonstration of oncogenic high risk human papilloma virus DNA and HPV-E7 protein in oral cancers. *Int J Immunopathol Pharmacol*. 2011;24(2 suppl):95-101.
37. Pannone G, Serpico R, Contaldo M, Longo F, Ionna F, Papagerakis SM. O81: site by site percentage and topographical pattern of lymph-node metastases in 174 neck dissections from 230 oral cancer patients. *Oral Oncol Suppl*. 2009;3:83. <http://dx.doi.org/10.1016/j.oos.2009.06.166>.
38. Di Domenico M, Pierantoni GM, Feola A, et al. Prognostic significance of N-Cadherin expression in oral squamous cell carcinoma. *Anticancer Res*. 2011;31:4211-4218.
39. Contaldo M, di Napoli A, Pannone G, et al. Node metastases features prognostic implications in OSCC: a retrospective study on 121 neck dissections. *Oncol Rep*. 2013. [Epub ahead of print; doi: 10.3892/or.2013.2779].

*Reprint requests:*

Maria Contaldo, DMD, PhD  
Multidisciplinary Department of Medical-Surgical and  
Odontostomatological Specialties  
Second University of Naples  
Via Luigi De Crecchio 6  
80138 Naples  
Italy  
[maria.contaldo@gmail.com](mailto:maria.contaldo@gmail.com); [maria.contaldo@unina2.it](mailto:maria.contaldo@unina2.it)